國立臺灣大學理學院化學所

碩士論文

Department or Graduate Institute of Chemistry
College of Science
National Taiwan University
Master Thesis

電極輔助噴灑游離法的開發及對生物分子的應用

Development of Electrode-Assisted Desorption Electrospray Ionization and Its Biomedical Applications

王鈺雯
Yu-Wen Wang

指導教授：陳仲瑄 博士
Advisor: Chung-Hsuan Chen, Ph.D.

中華民國 99 年 7 月
JULY, 2010

ACKNOWLEDGEMENTS

The author gratefully thanks Professor Chung-Hsuan Chen for guidance, Professor Abdil Özdemir; a visiting scholar from Sakarya University for the help and encouragement, Department of Chemistry, NTU for the great care of students. I also like to give thanks to senior members in the lab for listening, comforting and encouraging me when I got stuck, upset and lost confidence in research. In the past two years, I have learned a lot, not only in research but also the skill to get along well with colleagues and outside people.

中文摘要

大氣壓力游離法這幾年在質譜學領域逐漸的受到重視，因爲具有不需樣品前處理的優點。大氣壓力游離法可以直接將大氣中的固體與液體用於質譜分析。在此論文中、我們發展了電極輔助噴灑游離法（EADESI）、它可以直接用於生物樣品的快速分析。EADESI 是一種新型的大氣壓力游離法，可以檢測樣本在導體或非導體的樣品盤上。該儀器由三個主要部分：三維移動的樣品盤，高電壓電極，ESI 噴霧源。ESI 噴霧源以 45 °輕靠在電極旁邊。被霧化的溶劑氣體被電極極化後噴灑至樣本上，然後分析物離子化並隨著氣流被引入質譜儀中進行分析。我們的研究結果表明，EADESI 的空間解析度可以達到 25μm。 EADESI 可以對不同的生物樣本有廣泛的線性分析範圍、所以是一個可靠而嶄新的生物樣品分析方法。

Key words: 大氣壓力游離法、電極輔助噴灑游離法

ABSTRACT

Ambient ionization mass spectrometry has recently played an important role in Biological Mass Spectrometry because pre-treatment of samples is not required. It can be used for direct analysis of solid and liquid samples with a simple mass spectrometer. We developed the novel Electrode-Assisted Desorption Electrospray Ionization (EADESI) method for quick biomedical sample analysis. EADESI is a novel ambient ionization method which can be used as detection of samples on nearly any type of substrate. The instrument consists of three major parts: a three-dimensional movable sample plate with ground potential, a high voltage electrode, and a spray source. The spray source and electrode are positioned at about 45° with respect to each other and directly above the sample plate. Solvent nebulized by gas was used as a spray device to spray onto the sample, and then the desorbed analyte ions were introduced into the mass spectrometer. Our results indicated that EADESI can have space resolution of 25 μm. EADESI also has a wide dynamic range for different types of biomedical compounds.

Key words: Ambient ionization, Electrode-Assisted Desorption Electrospray Ionization

CONTENTS

LIST OF TABLES

LIST OF FIGURES

INTRODUCTION

I. AMBIENT IONIZATION MASS SPECTROMETRY

Ambient ionization mass spectrometry is defined as mass spectrometric analysis with no or minimal effort for sample preparation, using direct sampling and ionization at ambient conditions[1] .

Atmospheric pressure ionization (API) sources, such as electrospray ionization (ESI) and matrix-assisted laser desorption ionization (MALDI), have been considered as great achievements in the field of mass spectrometry, based on their efficient ways to analyze biomedical samples. Nevertheless, most API sources need external sample-preparation processes including dissolving samples in liquid, desalting and co-crystallization of samples with matrix.

Ambient ionization mass spectrometry, on the other hand, often requires no sample preparation and chemical separations[2]. In this case, samples can maintain their original chemical/physical/biological status[3]. This improvement can expand the utility of ambient ionization mass spectrometry for imaging, security check, drug discovery, etc.[2].

Another advantage is in situ detection. It also provides the possibility to obtain mass spectral images in the atmosphere[4].

Since Desorption electrospray ionization (DESI) was invented by R. G. Cooks in 2004[5], a number of pioneering scientists have developed creative ideas in this area due to the potential for broad applications(Table 1)[6]. Table 1 showed the statistical data of ambient ionization methods that have been developed in recent years.

Table 1. Chronology and perceived impact of developments in ambient ionization MS[6]

Method name	Acronym or abbreviation	Year of introduction	research papers [a] (papers/years)
Desorption electrospray ionization	DESI	2004	188(31)
Surface sampling probe	SSP	2004	5(1)
Direct analysis in real time	DART	2005	65(16)
Atmospheric solids analysis probe	ASAP	2005	7(1.4)
Electrospray laser desorption ionization	ELDI	2005	6(1.5)
Fused droplet electrospray ionization	FD-ESI	2005	2(0.5)
Direct atmospheric pressure chemical ionization	DAPCI	2005	89(22)
Matrix-assisted laser desorption electrospray ionization	MALDESI	2006	8(2.7)
Jet desorption electrospray ionization	jeDI	2006	1(0.3)
Extractive electrospray ionization	EESI	2006	22(7)
Desorption sonic spray ionization	DeSSI	2006	2(0.7)
Atmospheric pressure thermal desorption ionization	APTDI	2006	3(1)
Helium atmospheric pressure glow discharge ionization	HAPGDI	2006	1(0.5)
Plasma-assisted desorption ionization	PADI	2007	1(0.5)
Dielectric barrier desorption	DBDI	2007	2(1)

ionization			
Neutral desorption extractive electrospray ionization	ND-EESI	2007	5(2.5)
Laser diode thermal desorption	LDTD	2007	1(0.5)
Laser ablation electrospray ionization	LAESI	2007	1(0.5)
Desorption atmospheric pressure photo-ionization	DAPPI	2007	2(1)
Infra red laser ablation electrospray ionization	IR-LAESI	2008	7(3.5)
Flowing atmospheric-pressure afterglow	FAPA	2008	2(2)
Easy ambient sonic spray ionization	EASI	2008	5(5)
Remote analyte sampling transport and ionization relay	RASTIR	2008	1(1)
Laser ablation flowing atmospheric-pressure afterglow	LA-FAPA	2008	5(5)
Low temperature plasma	LTP	2008	7(7)
Desorption electrospray matastable-induced ionization	DEMI	2009	1(-)
Liquid micro-junction surface sampling probe/electrospray ionization	LMJ-SSP/ESI	2009	3(-)
Surface activated chemical ionization	SACI	2009	1(-)
Single particle aerosol mass spectrometry	SPAMS	2009	1(-)

[a] Approximate number of research articles found using SciFinder (v2007.2s) to November, 2009. These data include peer-reviewed papers (including web-based or in-press versions) and patents, but exclude review articles. Number of articles per year for each technique (shown in parentheses) provides an estimate of normalized output since first disclosure, except where the technique has been published for less than one year, which would greatly skew comparison of publication rate.

II. DESORPTION ELECTROSPRAY IONIZATION

Desorption electrospray ionization (DESI)[5] is the most well-known ambient ionization method. DESI combines an electrospray source with desorption ionization. In DESI, an incident spray impacts a surface leading to the desorption of analyte species into the gas phase for subsequent analysis by a mass spectrometer (Figure 1)[7]. In the DESI process, a spray of charged micro-droplets is directed towards the object or analyte on the sample plate in an ambient environment. The droplets impact the sample surface and lead to desorption of the analyte into the gas-phase. Then the ions are subsequently transported into the mass spectrometer. During the experiment, all parameters are critical. They include angle α (about 55°), angle β (~10°), voltage applied to the capillary tip, flow rate, gas pressure etc.

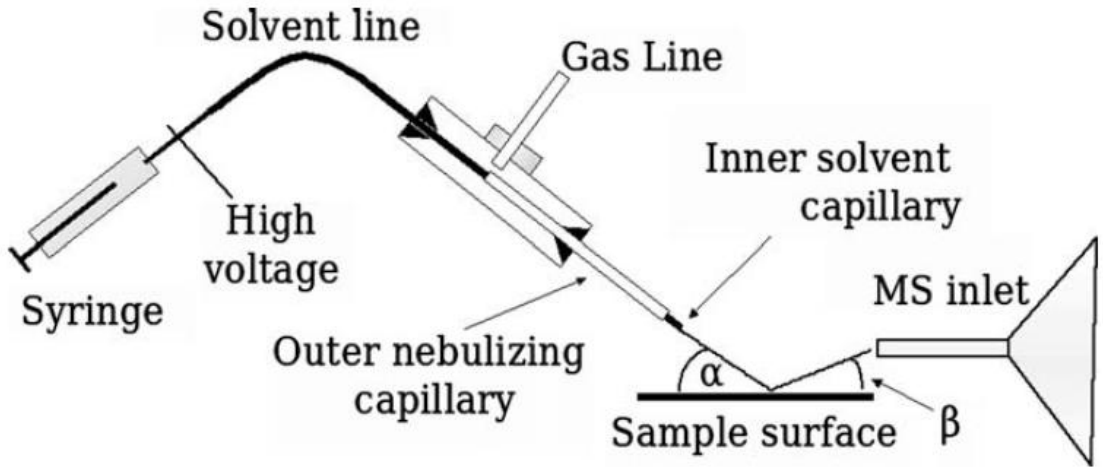

Figure 1. Typical DESI experimental configuration[7].

In DESI, the major mechanism involved has been named “droplet pickup”[7] of the analyte with subsequent solvent evaporation leading to the formation of analyte ions during transfer to the mass spectrometer. Cooks applied Phase Doppler Anemometry (PDA) to indicate the average sizes and velocities during the process[8]. Then they used continuum transport theory and finite volume computational fluid dynamics (CFD) to simulate the transport and collision processes and made spray and fluid velocity illustration[9](Figure 2). Figure 2 shows the simulation of the fluid transport from the nebulizing gas at the DESI sprayer and the motion of droplets after collide with the substrate surface. The color bar in Figure 2 means the velocity magnitude of the surrounding fluid. Droplets are represented as black spheres. The fluid motion in Figure 2 can be divided into two groups. First, the high altitude group is the larger droplets with great momentum. The droplets in this group could avoid the influence of sheath gas flow near the surface and the reflection angle is the angle. On the other hand, the second group is composed by smaller and faster droplets. The droplets in the latter group are driven across the surface by the fluid rate close to the surface has a “takeoff” angle of ~10°. It fit the experimental result that the highest ion signal is obtained when MS inlet is placed at a 10° angle to the surface and angle α is between 55-75°.

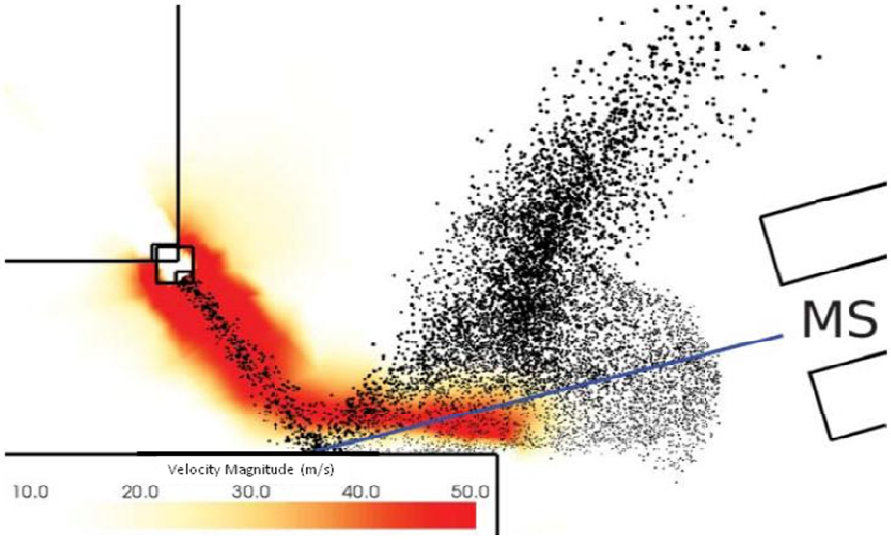

Figure 2. Spray and fluid velocity illustration of DESI[9]

Cooks and his coworkers provided the data to support a multi-stage momentum transfer method. These studies showed that surface wetting by the solvent spray out of capillary subsequently forms a thin film on the sample surface, effecting extraction of the condensed phase analyte into the surface film. They named this process ‘solvation delay ', which means the time taken to wet and then splash the solvent with analyte off of the sample plate. The momentum transfer from impacting droplets to the surrounding gas provides the energy needed to transport ions into the mass spectrometer inlet. In this process, the angle and distance of spray and entrance of MS are critical. Cooks also used the Navier-Stokes equations as a physical chemistry model (fluid dynamics) [7]. Figure 3 and Figure 4 show the time evolution of the fluid dynamic model of DESI with a spray angle of 55°. Figure 3 is a time series of droplet contours for the angle α =55° case. Time t is the time after droplet begins moving toward the surface. The small, fast droplets are initially produced when t=0.4μs and the droplets travel with small value of angle β. The larger, slower droplets splash out from the bulk fluid at the later time step

in the simulation. Figure 4 is the side view of the contours when t=0.4μs. The velocity vectors (glyphs) are placed on randomly selected cells. The phase in the simulation is presumed between liquid and gas. Figure 4 also shows the velocity and angle β of small droplets[7].

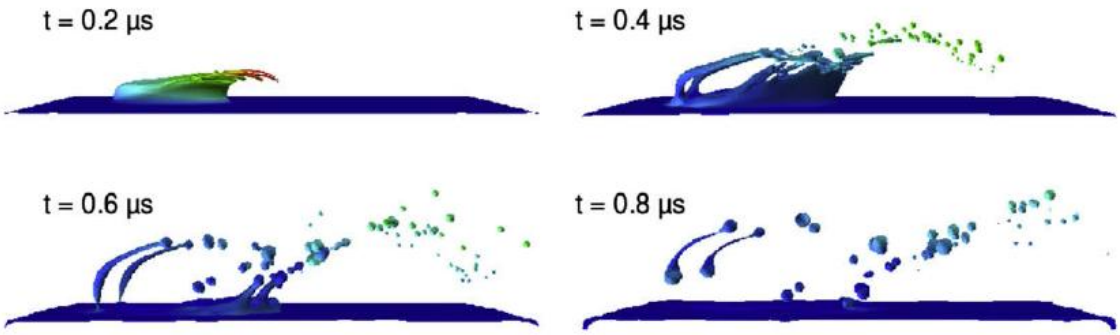

Figure 3. Contours of the indicator function at four simulation time steps simulation[7]

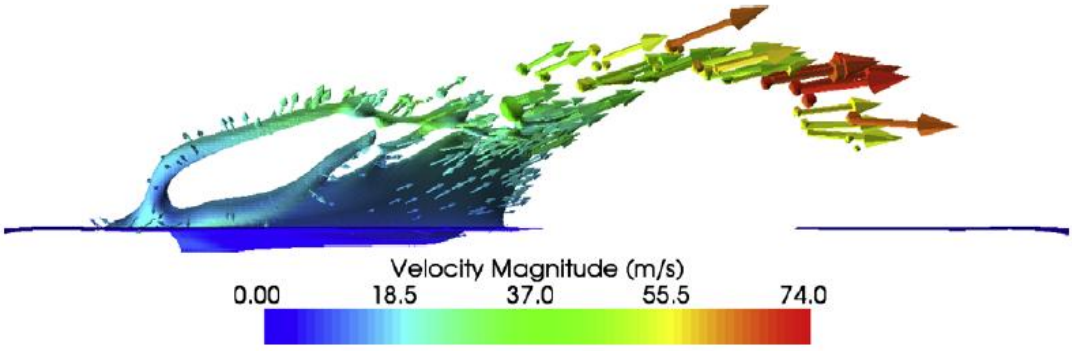

Figure 4. Side view of contours at t=0.4μs. [7]

DESI has many positive characteristics such as high analysis speed, soft ionization, production of both positive and negative ions, high sensitivity, high accuracy, etc[10]. Nevertheless, there are still some disadvantages for the technique and improvement is needed. These disadvantages include the analyte washing effect[11](Figure 5) and the resulting ill-defined sampling area.

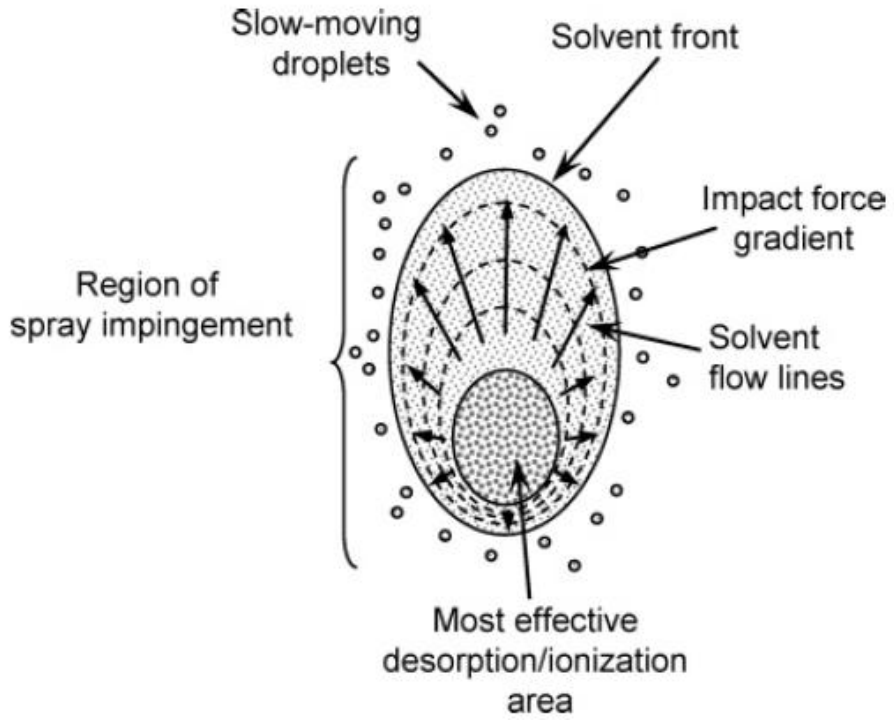

Figure 5. Idealized representation of the DESI impact plume region[11]

The inner region of the plume/sample interaction area is the impact area where the spray density is the highest. It is the most effective desorption/ionization region. The second zone is the result of solvent flow caused by diffusion from the inner region. The outer region consists of large, slow-moving droplets on the periphery of the larger impact region. The latter two regions are less effective in generating gas phase ions from the analyte on the surface. The droplets from the spray continuously impact these

wetted areas where splashing, jetting, and secondary droplet formation are the main physical processes present when droplets impact onto wetted films.

III. DIRECT ANALYSIS IN REAL TIME

Direct Analysis in Real Time (DART) was development by Laramee and Cody in 2005[12].

The basic DART source (Figure 6) is a tube that is divided into a number of smaller chambers. The gas used, such as nitrogen or helium flows through the tube. The gas passes through the first discharge chamber with an electrical potential of several kilovolts applied across it, producing electrons and molecules in excited states. Then the carrier gas passes through the second chamber to remove the un-desired ions. The third region which constitutes the perforated electrodes or grids can optionally heat the gas flow. Gas exiting through the third region is directed toward the sample and ions are subsequently introduced into mass spectrometer for analysis. The main function of the insulating cap is to protect the sample so that it does not touch the grid directly. The grid serves several functions: it acts as an ion repeller and it serves to remove ions of the opposite polarity thereby preventing signal loss by ion-ion recombination. Electrons can also be produced by surface Penning ionization and by oxidation of Rydberg atoms and molecules present in the gas flow. Gas flow could interact with liquid, solid or vapor-phase sample. Either direct or reflected, DART gas enters the MS inlet. In the DART, the distance and the angle of DART with respect to the sample surface affect the performance, but are not critical. Basically, DART can desorb and ionize sample located a distance of over 1 m from the air emitter.

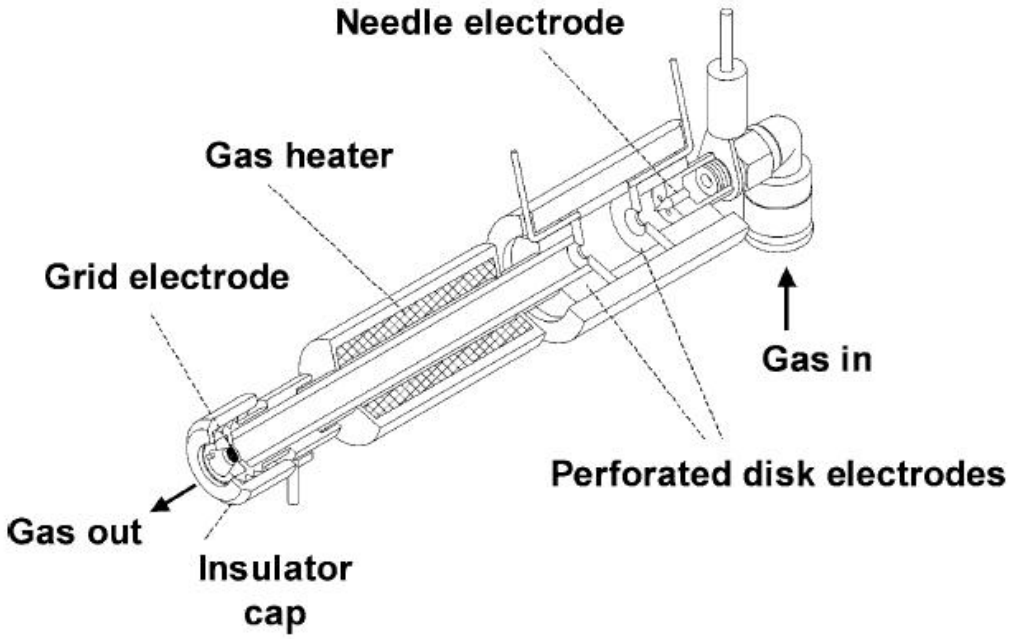

Figure 6. Cutaway view of the DART source[12]

The constitution of the whole experiment is as follows: in the first chamber, a gaseous discharge is formed by applying a +1 to+5 kilovolt potential difference across the needle and the perforated grounded disk. After passing through the perforated disks and a heated tube, the polarity of the ions exiting the device is determined by the potential of the grid electrode biased to a positive or negative potential[12]. The gas flow rate is ~1 L/min, and the temperature is ~ 250 ° C.

The ionization process involves an interaction between the reactant molecules (S) and electronically excited atoms or metastable species – M*:

$$M^* + S \rightarrow S^{+*} + M + e^-$$

Energy transfer occurs between the excited gas molecule (M*) and the surface of the neutral reactant molecule (S) when they collide. This causes an electron to be released from the reactant molecule, producing a radical cation. These excited gas

species collide with the sample surface and travel to the mass analyzer along with the gas stream (typically N_2 or Ne), resulting in an energy transfer to the neutral analyte molecule.

When He metastable atoms collide with an atmospheric pressure water molecule, the water molecule is ionized by the following process:

$$He(2^3S) + H_2O \rightarrow H_2O^{+*} + He(1^1S) + e^-$$

The ionized water molecule then undergoes several reactions with other neutral water molecules resulting in the formation of a protonated water cluster:

$$H_2O^{+*} + H_2O \rightarrow H_3O^+ + OH^*$$

$$H_3O^+ + nH_2O \rightarrow \left[(H_2O)_n H\right]^+$$

The water cluster then interacts with the analyte molecule (S) generating a protonated molecule.

$$\left[(H_2O)_n H\right]^+ + S \rightarrow SH^+ + nH_2O$$

DART can also operate in the negative ion mode by which negatively charged species are formed. The negative ion formation process is under current discussion and investigation.

DART also has disadvantages including the use of an internal standard when measuring the amount of sample present, difficulty determining the resolution, and the m/z range is limited, therefore, much improvement to this type of ionization source is needed.

IV. ELECTROSPRAY-ASSISTED LASER DESORPTION IONIZATION

Electrospray-assisted laser desorption ionization mass spectrometry (ELDI-MS)[13-16] (Figure 7)was developed by Shiea and co-workers. ELDI combines laser desorption with post-ionization of desorbed neutrals by electrospray ionization. This technique has been applied to the rapid analysis of solid materials under ambient conditions.

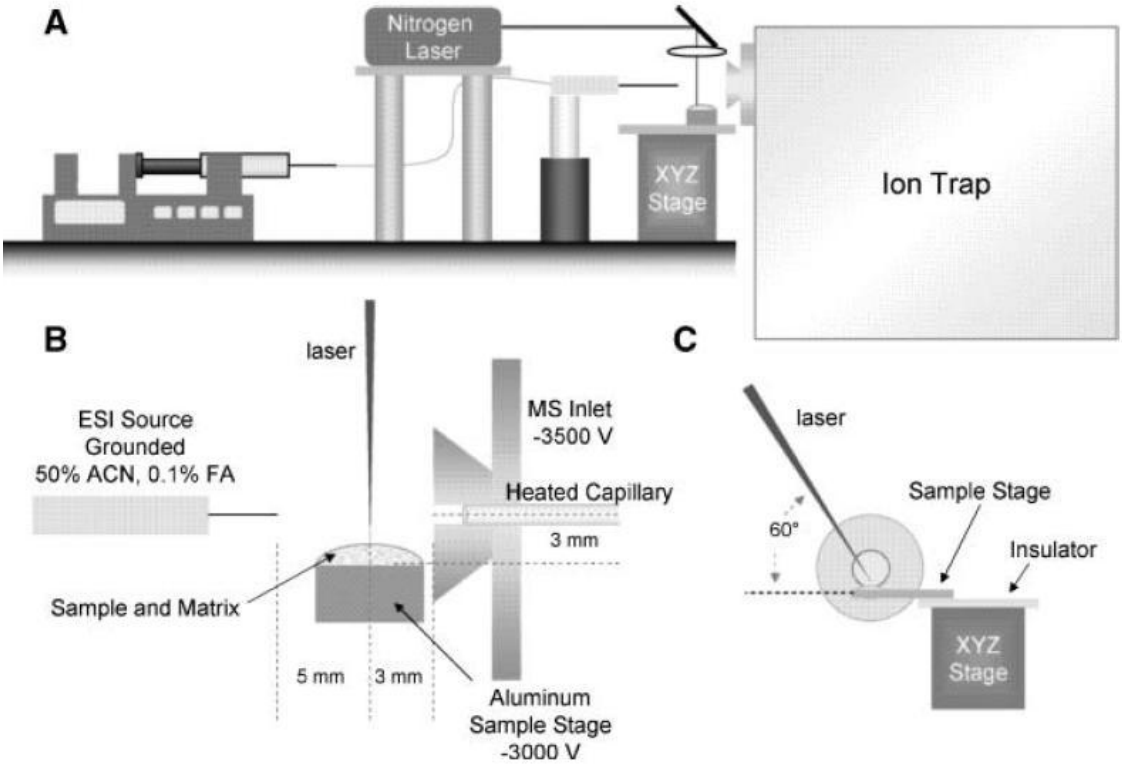

Figure 7. Schematics of the ELDI platform: (A) overall configuration of the ELDI source with the ion trap mass spectrometer, (B) side and (C) front view of the source.. [14]

ELDI typically applies a pulsed laser to desorb analytes from a translation stage and then ESI to produce ions (Figure 7B). UV radiation from a N_2 laser or a higher harmonic of a Nd:YAG laser is directed by two UV-grade, fused-silica prisms and focused onto the analyte drop. The incident angle of the laser beam onto the sample target was from 30°to 45°. The ESI emitter continuously sprayed solvent at a flow rate of 0.5–1.0 μL/min, at an applied voltage of 3.5 kV. ESI solvent was a mixture of acetonitrile (ACN)/deionized water in the ratio 1:1 v/v and 0.2% formic acid. The entrance of ESI MS was biased at -3.5 kV. An XYZ-stage aluminum sample plate was placed between the ESI source and the MS inlet, and biased at -3 kV to avoid the distortion of the electric field. Traditional ELDI samples usually involve protein aqueous solution (10–500 μM) mixed with matrix solution (10mg/mL in 50% ACN with 0.1% trifluoroacetic acid (TFA)) in the ratio 1:1 v/v. In general, 2-4 μL of the mixed solution is deposited to each spot on the sample plate.

ELDI is a soft ionization method for biological molecules.

Basically, the process can be separated into two major steps: In the first step, laser irradiation desorbs the analyte. In the second step, the desorbed analyte molecules are ionized by ESI. ELDI can be operated for both dry and wet biological samples, and with or without the need for traditional MALDI matrices. It can cover a wide mass range from angiotensin (1296 amu) to BSA (66,000 amu). The limit of detection (LOD) by ELDI-MS was reported as 23 ng/mm^2 for bovine carbonic anhydrase, a 29 KDa amu protein.

ELDI generates multiply charged ions. Therefore large biomolecule analysis by mass spectrometry can be easily achieved due to the low m/z. ELDI combined with tandem mass spectrometry can give the sequence information of proteins and DNA fragments by top-down analysis. Matrix is not essential for ELDI. IR-ELDI has also

been reported[15]. The water is the most efficient matrix when an IR is used for desorption.

V. DIELECTRIC BARRIER DISCHARGE IONIZATION

Dielectric Barrier Discharge Ionization (DBDI)[17-18] is a direct desorption/ionization technique for mass spectrometry that does not require any sample preparation. DBD is the electrical discharge between two electrodes separated by an insulating dielectric barrier. Originally called silent discharge and also known as ozone production discharge or partial discharge, it was first reported by Ernst Werner von Siemens in 1857[19] . The dielectric limits the average current density in the gas space, forming a stable, low-temperature plasma with high energy electrons[17] . Desorption/ ionization of analyte is achieved through the formation of a plasma sheath from the surface.

Figure 8 shows the configuration of DBDI. A high voltage is applied to the hollow stainless steel needle and the carrier gas is passed through the hollow tube. The sample plate usually is glass coated with a thin film of copper. The stainless steel needle and the copper sheet serve as two electrodes with ac voltage of 3.5–4.5 kV at frequencies of 18.0–25.0 kHz applied between them. The gas flow rate is typically set at 50–200 ml/min. The distance between the needle tip and the surface of the glass slide is about 5–10 mm, and the angle is set at 80–90°. The sample is desorbed and ionized in the resulting electric field. The distance between the DBDI source and MS inlet is typically set at 20-30 mm.

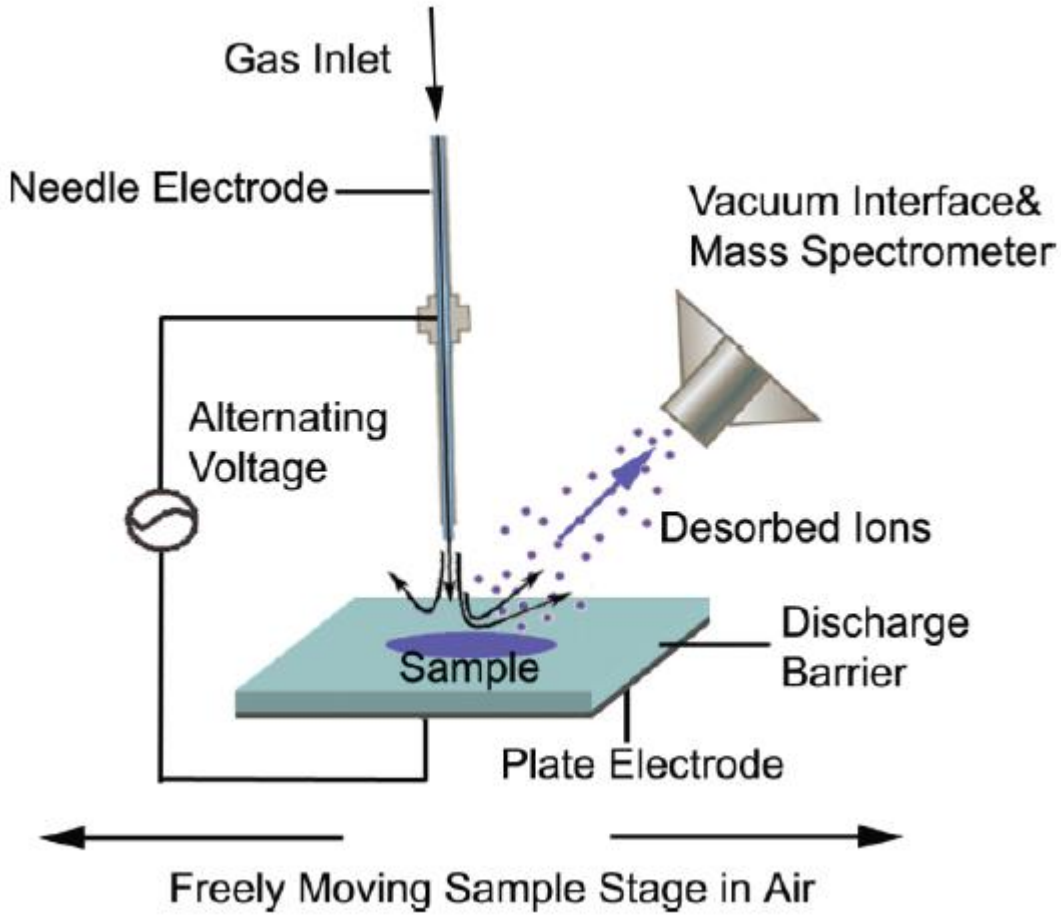

Figure 8. The schematic diagram of the DBDI ion source[17]

The ionization yield is a strong function of the air flow, proton affinity, and the type of analyte molecules sampled. The ionization mechanism has been speculated as similar to fast atom bombardment, electron impact ionization, and charge transfer. Further studies are needed to reveal the detailed mechanism.

DBDI is simple, small, and suitable for portable MS. But it still needs further development for the ionization of large molecules.

VI. ELECTRODE-ASSISTED DESORPTION ELECTROSPRAY IONIZATION (EADESI)

Because the ambient ionization method has so many advantages: in terms of minimal effort for sample preparation, and direct sampling and ionization under ambient conditions, developing a new and better ambient ionization method especially for biomolecule detection, would be especially useful. In this work, we developed electrode-assisted desorption electrospray ionization (EADESI) to provide further improvement in terms of simplicity and spatial resolution, and investigated the utility of adding matrix to the sample to enhance signals in terms of intensity.

The instrument consists of three major parts: a three-dimensional movable, grounded sample plate, a high voltage electrode, and a spray source. The spray source and electrode are positioned at an angle of ~45° and directly located above the sample plate. Solvent pressured by gas was used as the spray device to spray onto the sample, the desorbed analyte ions being subsequently introduced into the mass spectrometer.

METHOD

ELECTROSPRAY IONIZATION (ESI)

The ESI-ion trap mass spectrometer used in this work is the Esquire 3000^{+} (Bruker Corporation, USA). We replaced the ionization source (electrospray) with a homebuilt EADESI source. The mass analyzer and ion detector remained in their original configuration. The Esquire 3000^{+} uses RF octupoles for ion focusing and transport to introduce ions into the ion-trap. A Daly detector was used for efficient detection of ions over a wide mass range.

EADESI

The whole EADESI mass spectrometer can be divided into four parts (Figure 9): electrode, spray tip, grounded sample plate and mass spectrometer (MS). The electrode was made of stainless steel with a diameter of 40μm, and the electrode tip was 20μm. A voltage of 250 ~ 1000 V was applied to the electrode, to produce optimum signals under different experimental conditions.

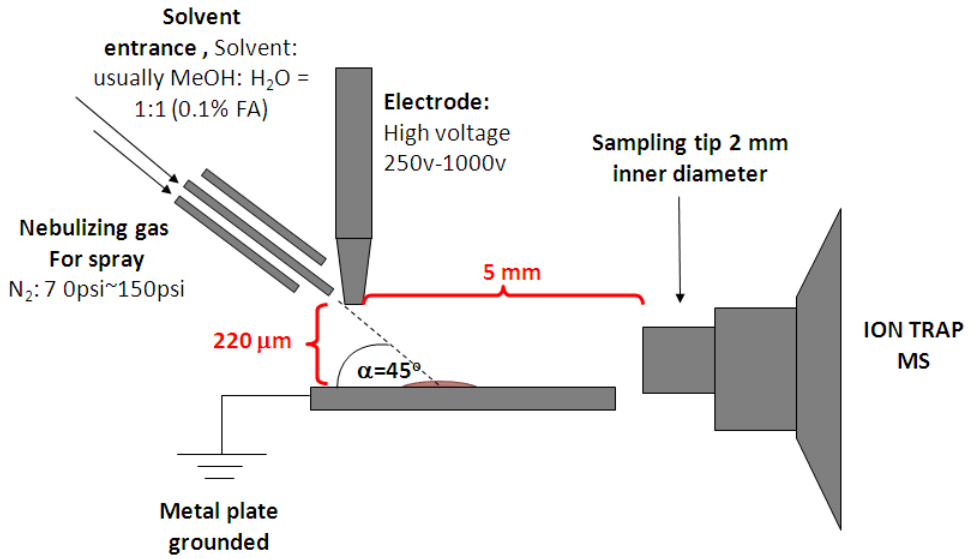

Figure 9. The Schematic of EADESI

The solvent was continuously introduced into the spray then nebulized by a high pressure nitrogen gas through a silica capillary (i.d. 40 µm). The flow rate was 30-100 µl/hour and the gas pressure was 70~150psi. Experiments were carried out using a commercial Omni Spray Ion Source Kit (Prosolia, Inc., IN) without connecting to the power supply. The spray emitter was made of fused silica with an inner diameter of 40µm and an outer diameter of 150µm.

A stainless steel platform was used to support a Teflon surface to isolate a metal sample plate from interactions with other metal surfaces. The sample plate was grounded, and a 10 MΩ resistor was placed between the plate and a grounding cable to prevent severe discharge between the plate and the HV-tip. The sample plate was adjustable in 3-dimensions.

We also designed an extension to the original MS inlet. The main purpose was to make the distance between sample and inlet shorter and use a larger bore inlet to increase the number of ions transported into the MS. The center of the MS inlet was ~70 μm above the sample plate. The entrance configuration was trapezoidal.

The relative positions of all components are shown in Figure 9. In general, the electrode was set above the sample plate vertically, the distance from the electrode tip to the surface was ~200μm (this distance can be adjusted, depending on several factors including sample type (crystal or powder), and the voltages applied to the electrode and sample plate). When all other parameters were tuned, the electrode and the MS inlet distance was 0.5cm.

The spray was placed on the right side of the electrode and the leading edge of the emitter slightly touched the electrode (Figure 10). The lower edge of the emitter was aligned with the tip of the electrode. The spray Impact angle (α in Figure 9) was 45°, meaning the angle at which the sprayed charge droplets from the outlet of the solvent capillary were directed towards the sample on the surface. The main reason that the spray was placed on the side of the electrode instead of behind the electrode is to avoid the solvent flow from hitting the electrode and being divided into two channels which might increase the sampling region.

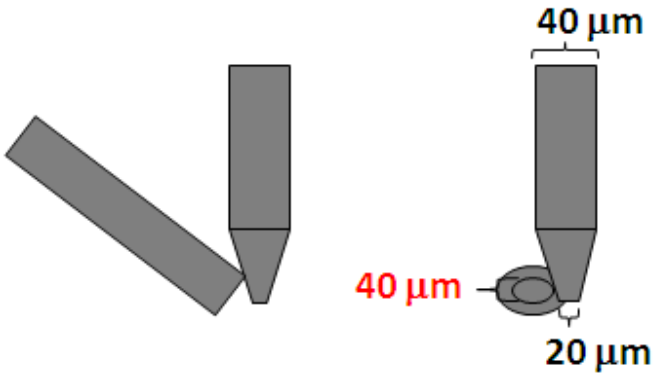

Figure 10. Relative Configuration of tip and spray

SAMPLE PREPARATION

Analyte compounds were dissolved in water at different concentrations. In general, solutions were diluted in methanol/water 1:1 (v/v) to the final concentrations of 10^{-2}; 10^{-3}; 10^{-4}; 10^{-5}; 10^{-6} M. 10μl of the sample solution was pipetted for each spot on the surface, and the spotting area was ~1cm^2.

Sinapinic acid(SA) solution with a concentration of $5x10^{-3}$ M was mixed with acetonitrile. Sample preparation processes were important for obtaining good spectra.

In this work, three different types of samples were prepared (Figure 11): (1) the sample solution of 10uL without matrix was deposited on the sample plate, (2) the samples were prepared by mixing 1:1 V / V of protein aqueous solution (10^{-2}M ~ 10^{-6}M) and matrix solution (10mg/mL in 50 % ACN) then the mixed solution of 10uL was deposited onto the sample plate, and (3) the matrix solution of 10uL was prepared and subsequently deposited on the sample plate, then analyte solution (10^{-2}M ~ 10^{-6}M) 10uL was added onto the matrix spot.

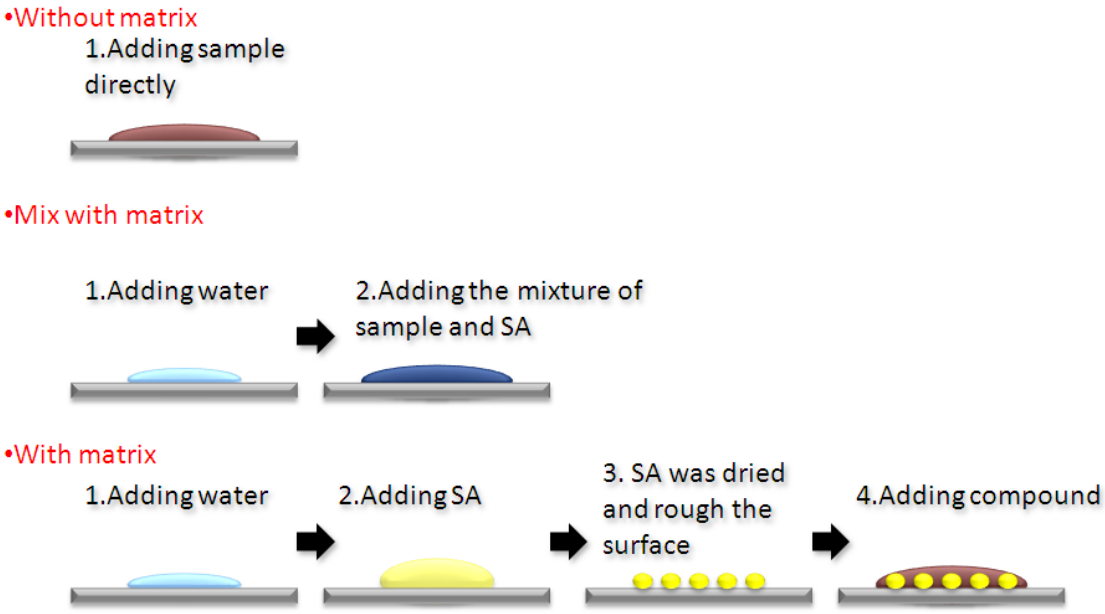

Figure 11. Sample Preparation

RESULTS AND DISCUSSIONS

DETECTION OF BIOMOLECULES

The EADESI technique can be applied to various samples. Different groups of analytes have been examined, including peptides, proteins, small sugars, drug molecules and human fluids such as urine and blood.

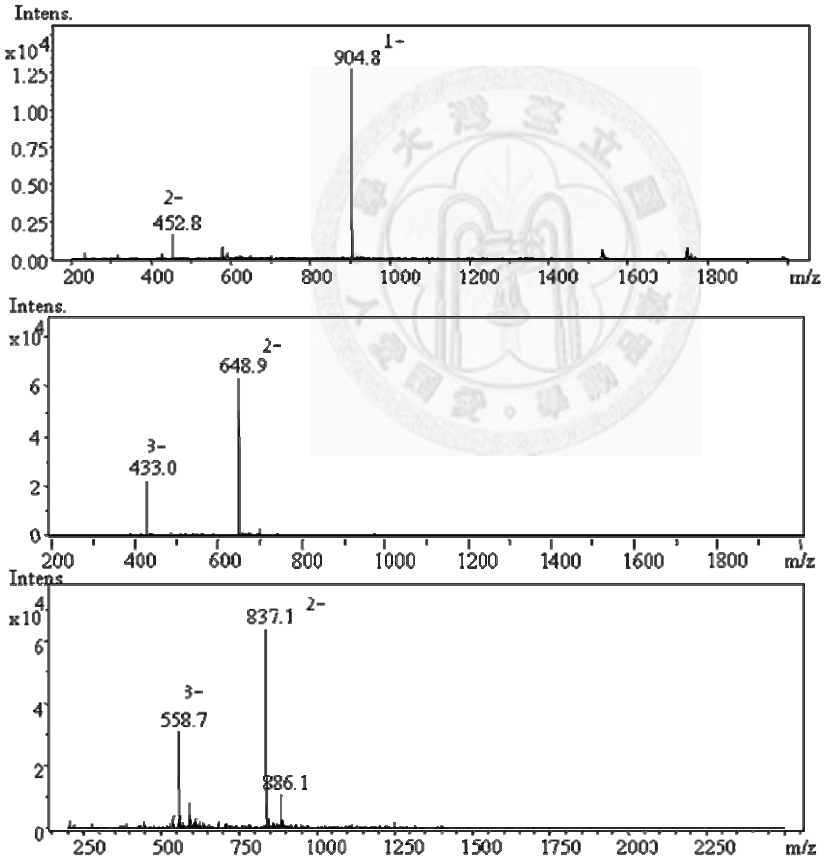

Figure 12. Mass spectra of (A)Bradykinin 1-8 ,(B)Angiotensin I and(C) Neurotensin.

In Figure 12, Figure 13 and Figure 14, the simple bimolecular analysis using EADESI are shown. For Bradykinin 1-8 acetate salt hydrate (M.W.= 904.02), the singly -charged ion (m/z 905) and doubly-charged ion (m/z 453) were detected; doubly- (m/z 649) and triply-charged ions (m/z 433) were observed for Angiotensin I (M.W.= 1296.48)and the doubly- (m/z 837) and triply-charged ions (m/z 559) also were detected for Neurotensin (M.W.= 1672.92)(Figure 12) in the positive ion mode. The observed charge numbers are very similar to those measured for the ionization of the corresponding compounds by ESI.

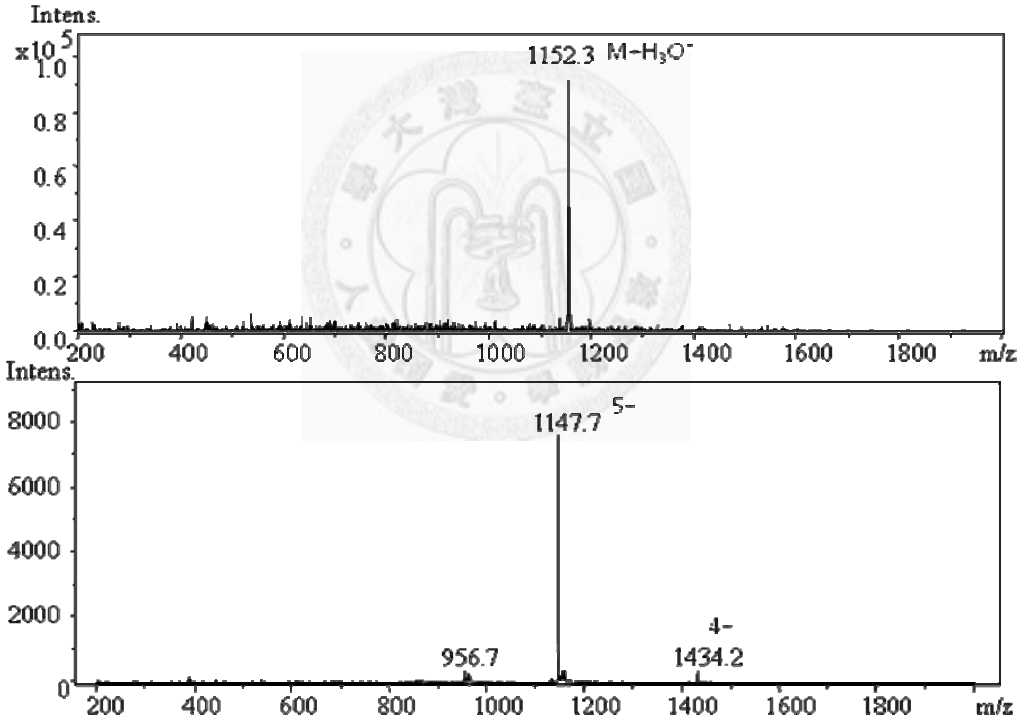

Figure 13. Mass spectra of (A)Beta-Cyclodextrin and (B)Bovine Insulin.

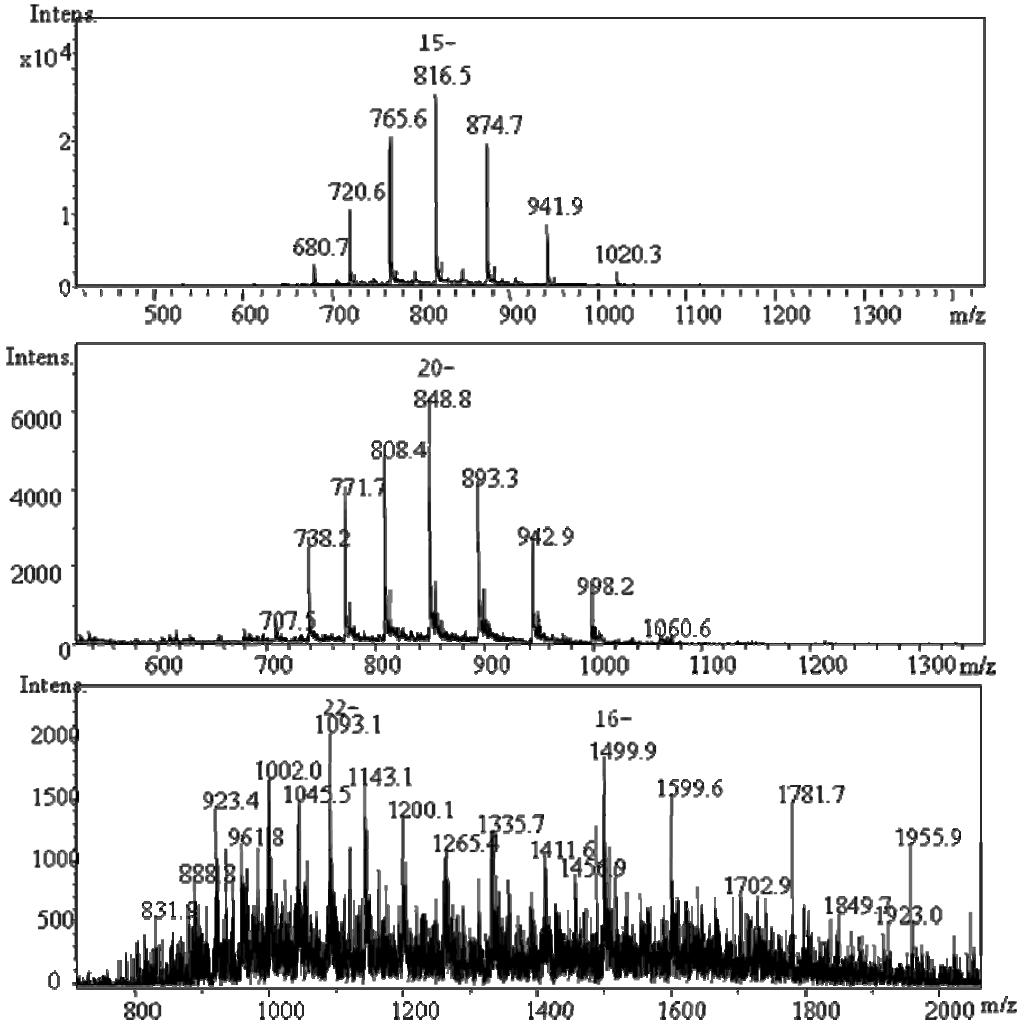

Figure 14. Mass spectra of (A)Cytochrome C, (B)Myoglobin and (C)Beta-Casein.

β-Cyclodextrin (M.W.=1134, seven sugar ring molecule) was detected in both positive and negative mode. In Figure 13(A), the molecule with hydronium ion attached ($M+H_3O^+$) was observed in positive mode. Figure 13(B) is the spectrum of Bovine Insulin (M.W. =5733.49), the most abundant peak is the 5+ charge state.

Figure 14 is the mass spectra for 12.9KDa Cytochrome C, 16.9KDa Myoglobin and 24KDa â-Casein. The multiply charged ion distributions in Figure 14 are similar to those observed by ESI-MS.

Human body fluid samples (Figure 15) can be directly analyzed by EADESI if the sample is dried on the metal surface. The EADESI mass spectra of dried blood and urine showed several peaks corresponding to the chemical constituents of these samples. Using EADESI, pretreatment of blood and urine samples is not necessary. The EADESI mass spectrum of dried blood in positive mode, showed the characteristic peaks for multiple charged α and β chains of hemoglobin (Figure 15A).

The EADESI method has also been tested on a non-prescription pharmaceutical formulation of PANADOL cold extra. The tablet formulation of this drug contains six different active ingredients of various amounts: acetaminophen 500 mg, phenylephedrine HCl 10 mg, terpin hydrate 33.3 mg, vitamin C 63.3 mg, caffeine 25 mg, and noscapine 15 mg(Table 2). The mass spectra obtained for PANADOL using the EADESI source are shown in Figure 15B. The protonated molecules for each of the active ingredients are shown and labeled in the EADESI mass spectra. Possibly ion suppression effects caused differences in the observed ionization efficiencies and signal intensities for each of the protonated ions of the individual active ingredients.

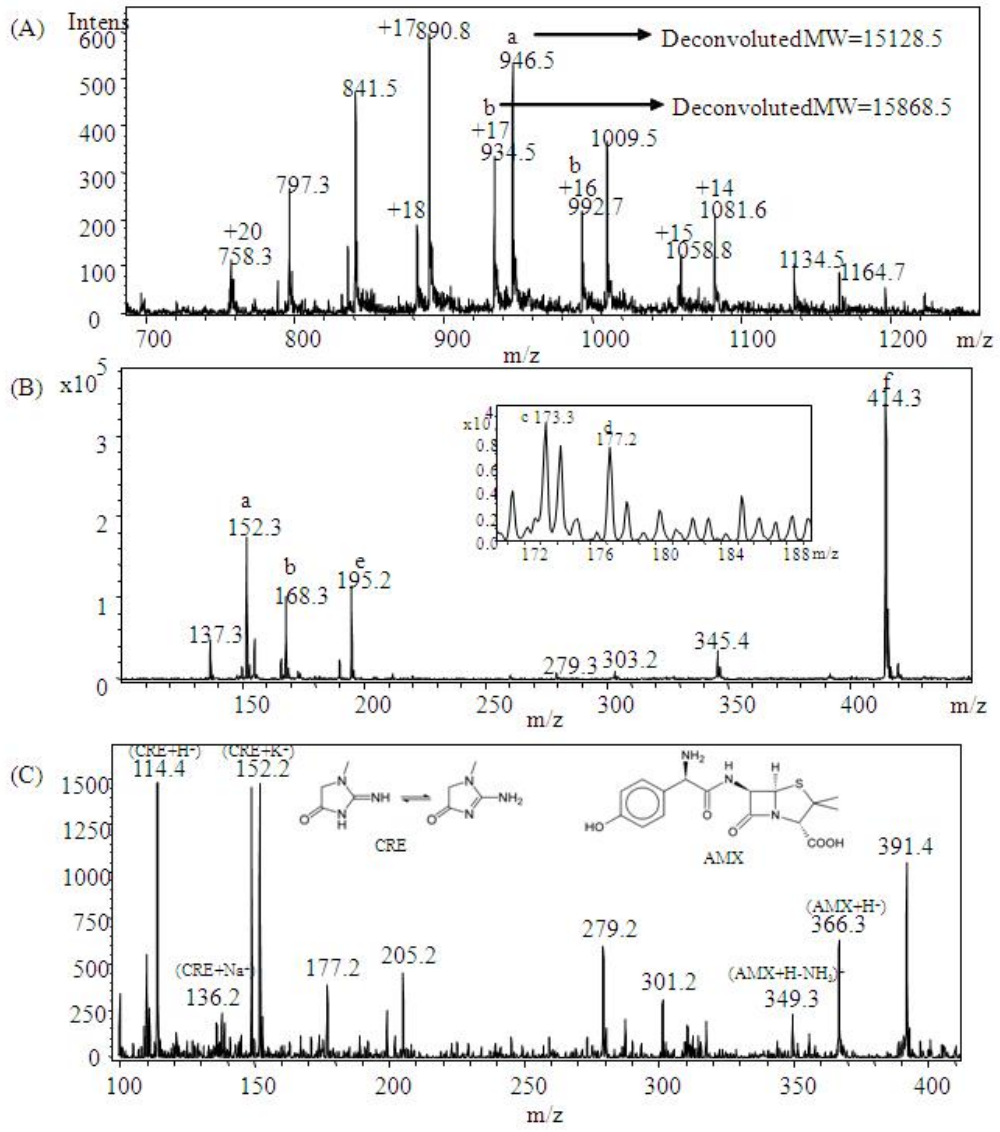

Figure 15. (A) Mass spectrum of a blood sample with a 1:10 dilution with distilled water. A 10-µl sample of the diluted solution was dispensed onto a SS surface and allowed to air dry. The spectrum shows ions corresponding to hemoglobin a and b chains. (B) EADESI analysis of the PANADOL commercial pharmaceutical. (C) Direct analysis of amoxicillin in human urine using EADESI without sample pretreatment.

Table 2. The component of PANADOL

	Chemicals	**Structure**	**Chemical Formula**
a	Acetaminophen	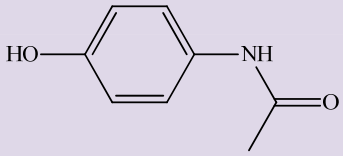	$C_8H_9NO_2$ Molecular Weight: 151.2
b	Phenylephedrine HCl	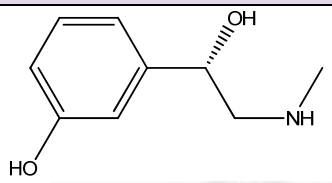	$C_9H_{13}NO_2$ Molecular Weight: 167.2
c	Terpin hydrate	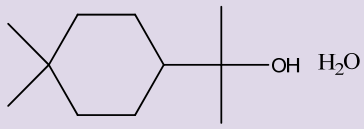	$C_{11}H_{24}O_2$ Molecular Weight: 188.3
d	Vitamin C	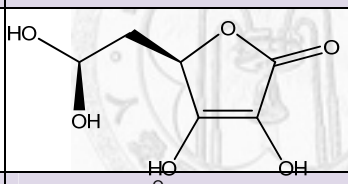	$C_6H_8O_6$ Molecular Weight: 176.1
e	Caffeine	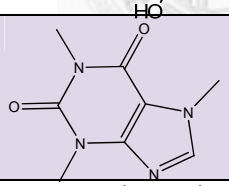	$C_8H_{10}N_4O_2$ Molecular Weight: 194.2
f	Noscapine	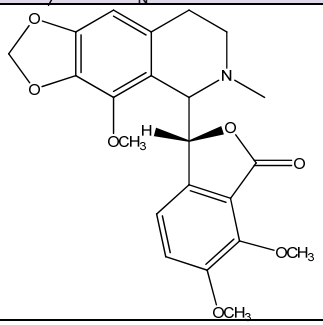	$C_{22}H_{23}NO_7$ Molecular Weight: 413.4

Analysis of Urine is a simple method to rapidly screen for drugs or drug metabolites. The use of ambient MS without pre-separation and desalting has been reported [20-23]. For drug analysis in human urine, samples were obtained 2 hours after the administration of 1000 mg of amoxicillin (AMX). EADESI was used to detect AMX in human urine by using a mixture of methanol/water/formic acid (1:1:0.01 by volume) flowing over the HV-tip. A 10-μl urine sample was dispensed onto the stainless steel sample plate. Figure 15C shows the positive ion mass spectrum obtained without any pre-treatment of the urine sample. Detected ions other than clusters have been assigned to protonated creatine (m/z 114), sodium-attached creatine (CRE) (m/z 136), and potassium-attached creatine (m/z 152). The protonated AMX parent ion and its signature fragment ions that formed by losing an NH_3 group appeared at mz/ 366 and 349, respectively. The high intensity signal of the ion $[CRE+K]^+$ (m/z 152), existed most of the time. This result strongly indicates a high tolerance of salts in samples when using EADESI mass spectrometry.

PARAMETERS OF EADESI

The parameters of EADESI play an important role in the analysis of the data obtained. The effects of various experimental parameters, including the applied voltage (Figure 16), flow rate (Figure 17) and the angle of spray (Figure 18) were examined.

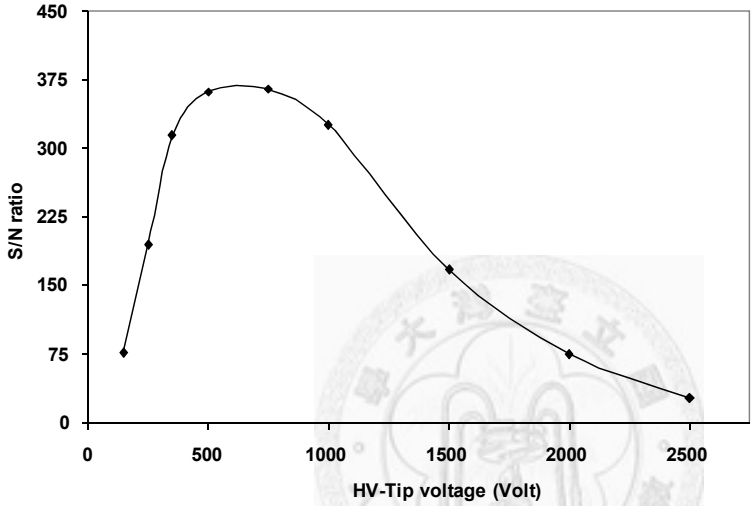

Figure 16. Voltage Dependent ionization of Angitensin I. S/N ratio of Angiotensin I signal versus voltage applied. The height of tip to the surface was 250 μm throughout the experiments.

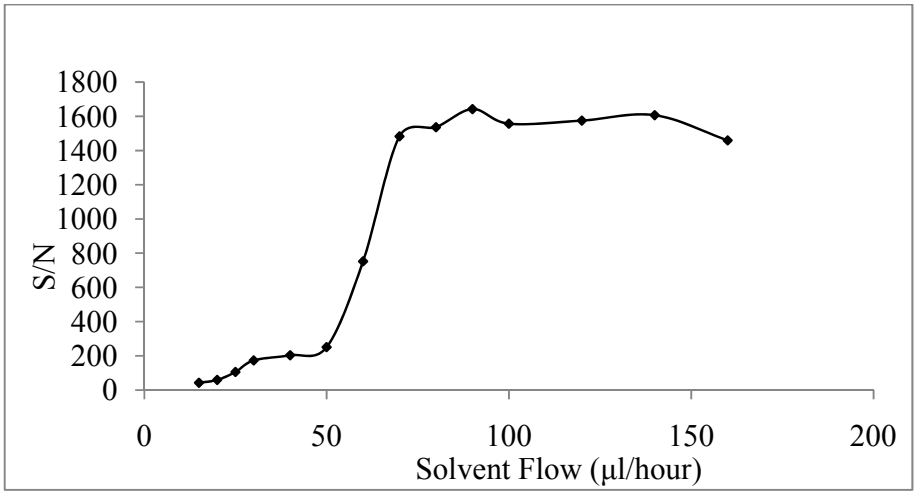

Figure 17. Signal/Noise versus Solvent Flow Rate

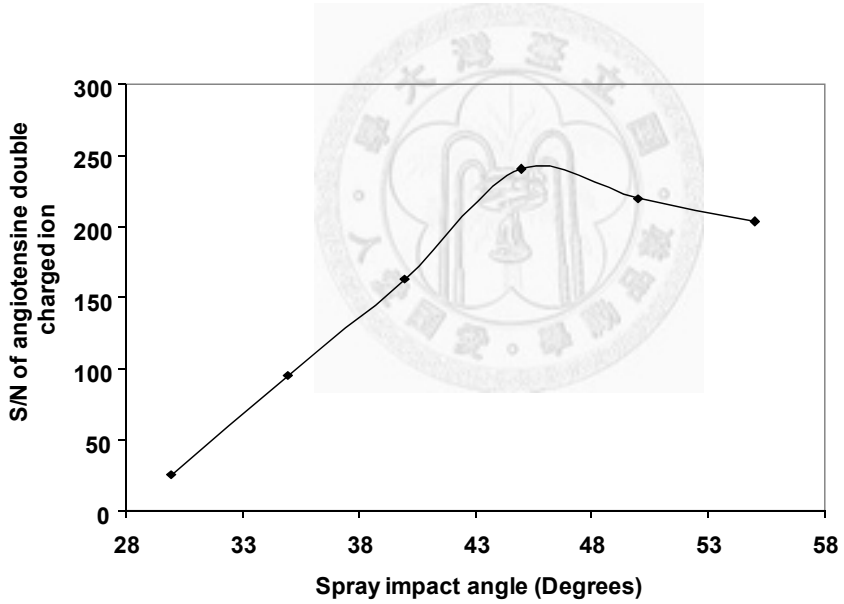

Figure 18. Angle Dependence for EADESI

Figure 16 shows the signal-to-noise ratio (S/N) versus the voltage applied to the electrode. The S/N has a maximum at ~750V. This maximum rapidly drops with a further increase in voltage. In fact, the optimum value depends on the distance between the

electrode and the sample plate. The optimum distance was found to be very close to the distance for the threshold for arcing with a fixed voltage. When the applied voltage is over 1000V and the tip is very near to the sample plate, strong arcing will appear between the tip and the sample plate. The noise increased due to the intense arcing, decreasing the S / N. On the other hand, the electric field can be too weak to efficiently ionize the analyte with a fixed distance between the tip and the plate when the voltage is too low.

Results in Figure 17 appear to be similar to the results from DESI[24]. When the flow rate is low, the droplet size is too small to produce analyte ions efficiently. With an increase of the flow rate, the size of droplets became appropriate for producing analyte ions and S/N increases. The increased S/N at higher flow rates may be due to more efficient desolvation. A higher flow rate would also increase the total amount of analyte ionized assuming a larger area is sampled.

Figure 18 shows the effect of the spray angle on S/N for EADESI. The spray angle affects the trajectories of droplets and ions. Droplets from the spray, passing by the electrodes, hit the sample plate and desorb/ionize the analyte chemicals. Different angles are expected to have different interaction efficiencies for dissolution and ionization of analytes. We found an angle between 45 ° ~ 50 ° usually gave the best S / N in our experiments.

SPATIAL RESOLUTION

Here, we define the spatial resolution of EADESI as the minimum area that can be probed reliably. It is important to evaluate the spatial resolution of the EADESI source for possible applications to molecular imaging.

The determination of spatial resolution was as follows: the position of the platform with a uniform distribution of sample was measured by moving in 50 μm increments per step, while using EADESI to detect the sample. In this experiment, Rhodamine B (M.W. =444) was used (Figure 19), without matrix. Figure 20 is a photograph of the sample plate taken after rastering the surface. As Figure 20 A shows, a light band indicates the sample has been completely depleted and the metal plate underneath is revealed. On the other hand, a dark band indicates the area where Rhodamine B is not depleted by EADESI. Both areas are approximately 25 μm in width. This result indicates that the spatial resolution was about 25 μm, which is better than the results reported by Kertesz and van Berkel[25]. With their setup, a spatial resolution of 40 μm was achieved only on specific substrates. We interpret our result as due to the high and more uniform electric field present between the grounded sample plate and electrode tip, reducing the spatial spread of the charged droplets transported to the sample plate. Therefore, compared to DESI, EADESI has a better spatial resolution.

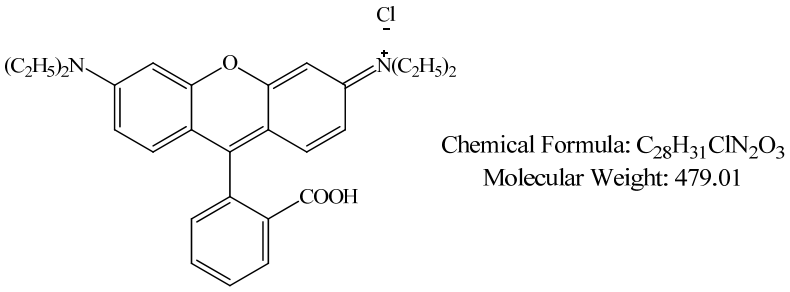

Figure 19. Structure of Rhodamine-B, the molecular weight of the cation is 443.23Da

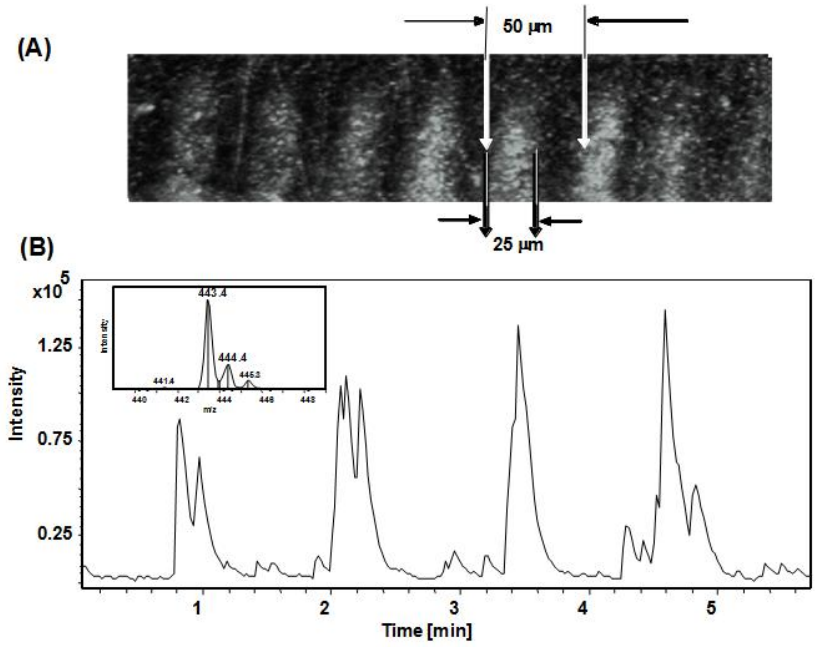

Figure 20. Resolution Study of EADESI: (A) the photo of sample plate after experiment (B) the experimental results for ion intensity vs. time.

Figure 20B shows the experimental results for ion intensity vs. time. The results were obtained from the following steps. At the start time, the first spot was probed by EADESI until the sample was depleted and the signal was significantly reduced. Then the sample

plate was moved 50μm to the next spot and the experiment was repeated. In Figure 20B, the signal intensity in the first minute was blank due to the area probe was detected had no sample. The probe was moved to the sample after one minute and the signal intensity increased. Then the spray tip remained in the same position until the signal was low and the background stable (the sample was exhausted). The tip was then moved to the next site, the intensity increased again, and the process was repeated. Therefore, the signal intensity from each spot remained relatively constant. The upper left picture in Figure 20 B was the correspondent mass spectrum with isotope well resolved.

Figure 21 shows another result for the measurement of spatial resolution. In this case the area probed is rectangular in shape, not round as obtained using DESI. The ratio of the length to width of the rectangular depleted areas is about 8:1as shown in Figure 21 (That is, when using EADESI the sampled areas are ~25 × (8 × 25) μm^2, or $5\times10^{-3} mm^2$). This value will be taken into account when measuring the detection limit of EADESI.

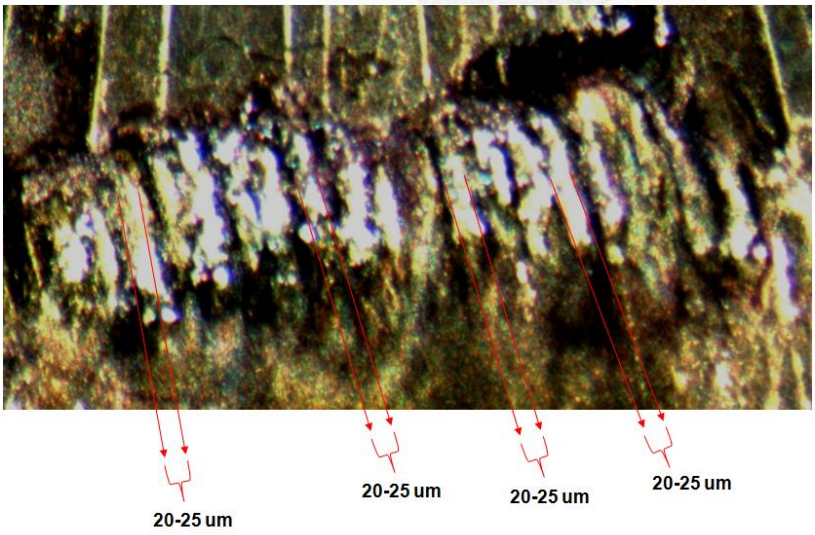

Figure 21. Spatial Resolution Study on a large scale

LIMIT OF DETECTION (LOD)

Table 3 shows the limit of detection (LOD) of some biological molecules (peptides and proteins) by EADESI. Limit of Detection (LOD), means the lowest amount of a substance that can be distinguished from the absence of that substance (a blank value) within a stated confidence limit. In mass spectrometry, we usually define LOD as the minimum amount of analyte to give signals with the S/N value equal to 3. In Table 3[24, 26], there were two different units of value presented, namely pg and pg/mm^2. The latter unit, pg/mm^2, was calculated by the concentration of the samples on the surface, this value showed the amount of chemical per unit area on the sample plate. We also calculated the total weight (pg) probed by EADESI. The analyte amount loaded on the surface multiplied the detection area, gives the total amount of sample probed by EADESI. Therefore, this is the minimum amount of analyte required for detection. However, it's impossible to prepare the sample in such small area which equal to detection area, so both value are important.

In this study, we detected proteins with different molecular weights, and compared the values with DESI. Two different experimental conditions were pursued: namely sample mixed with matrix and without matrix. Results from both conditions are quite good. Overall, as the molecular weight of the protein increased, the LOD also increased. For example, the LOD of Angiotensin in EADESI was 0.12pg, but increased to 9 pg for insulin.

The LODs for the samples without matrix are higher than those with matrix. It indicates that matrix can enhance the detection sensitivity for EADESI. The phenomena have not been reported in either ESI or DESI.

Table 3. Detection Limit of EASI[24, 26]

	METAL PLATE				DESI	
	WITH MATRIX		WITHOUT MATRIX			
	pg	**pg/mm2**	**pg**	**pg/mm2**	**pg**	**pg/mm2**
Bradykinin	0.003125	1			0.7	0.04
Angiotensin	0.075	24	1.5625	500	1.2	0.05
Insulin	5.625	1.8 ng/mm^2	37.5	12 ng/mm^2	150	30
Cytochrome C	9.375	3 ng/mm^2	13.8	4.42 ng/mm^2	500	40
Albumin	1856.25	594 ng/mm^2	18750	6000 ng/mm^2		4000 ng/mm^2 (From Basile)

LINEAR RANGE

The linear dynamic range is the range over which ion signal is linearly proportional to the analyte amount or concentration in the sample[27]. The most important significance of measuring dynamic range is that ESI and MALDI have been most used as a qualitative measure. Because of the unpredictability of ionization efficiency, MALDI MS is a poor technique to be used for quantitative measurement. Most quantitative measurements have been achieved with an internal standard present. Due to the importance of quantitative measurements, we attempted to make quantitative measurements using EADESI.

Tests of linear range were made for samples with and without matrix. We observed a linear relationship for angiotensin (Figure 22), insulin (Figure 23) and cytochrome C (Figure 24).

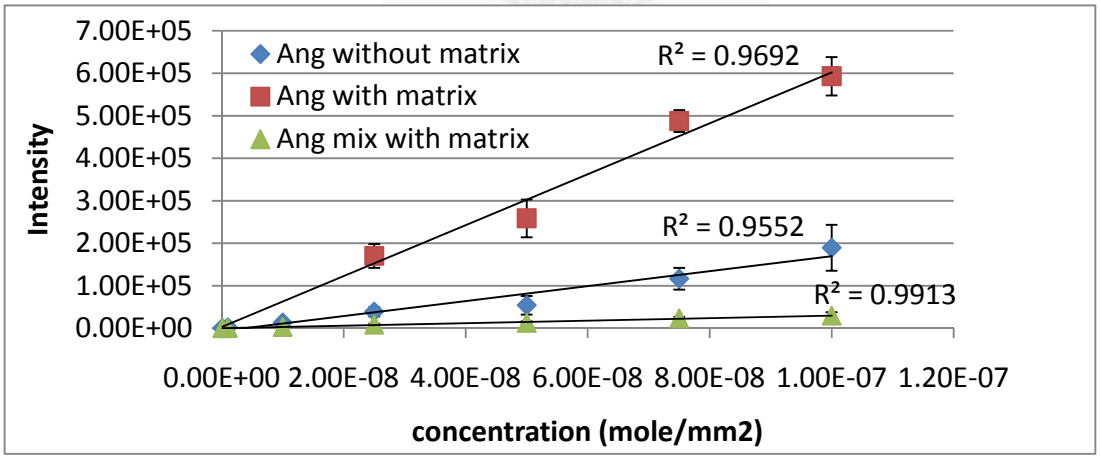

Figure 22. Signal intensity versus concentration of Angiotensin

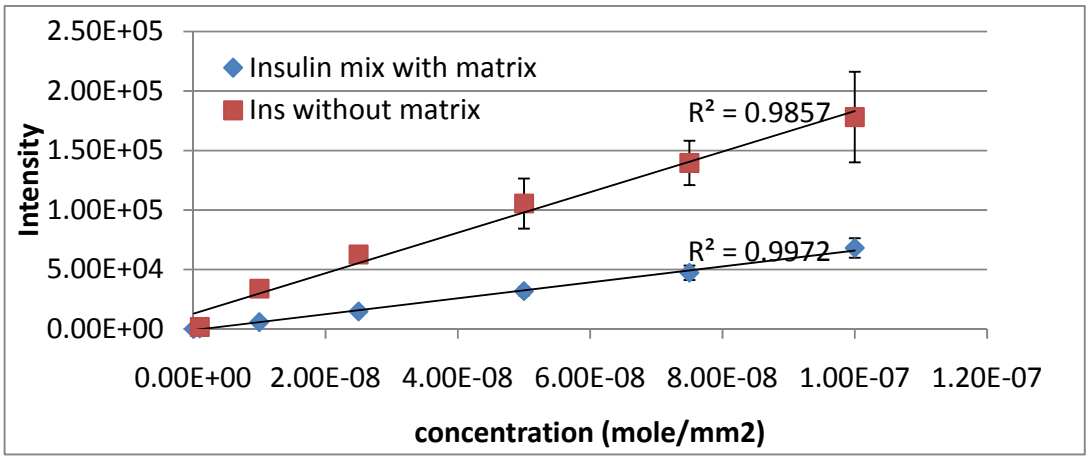

Figure 23. Signal intensity versus concentration of Insulin

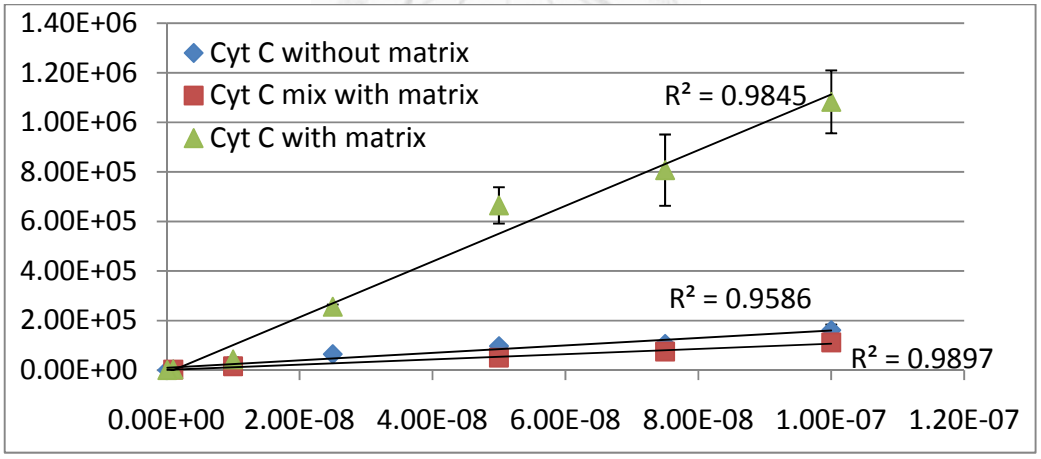

Figure 24. Signal intensity versus concentration of Cytochrome C

All R-square values obtained are greater than 0.95. This indicates the concentration and signal intensity are reasonably related. But in quantitative accuracy tests the relative standard deviations (RSDs) of EADESI was ~20 %. This implies that EADESI is not a

quantitative technique. This is perhaps because the sample is not uniformly spread over the surface.

Also, as shown in the Figure 22 and Figure 24, three different sample preparations were tested. Different sample preparation processes can give different concentrations on the surfaces. When pure analyte sample without matrix is placed on the surface, a thin film is formed. For EADESI, ionization is still possible and will give reliable results. When the sample is mixed with matrix, although a thin film is not formed as with a pure compound, the analyte signal fraction with respect to the total signal drops significantly, so lower signals are obtained. With matrix deposited on the sample plate first and adding analyte afterward, just as described in method section, a rough surface forms for the matrix and a thin film of analyte molecules dries on the matrix i.e., higher quality signals can be expected.

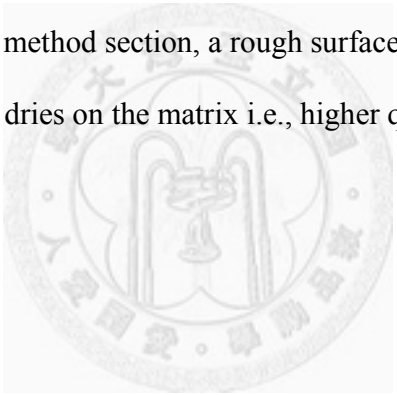

MUTIPLE CHARGING

There are no distinct differences between the spectra recorded by DESI and ESI in the case of small molecules. However, the charge state distribution shows clear differences in the results between the ESI and DESI spectra for large proteins [24, 28]. The results of EADESI show that the charge states formed for Myoglobin (Figure 25). The EADESI method shows a similar charge state distribution to ESI when applied to the larger proteins. That means the detection of proteins which have higher molecular weight would be possible.

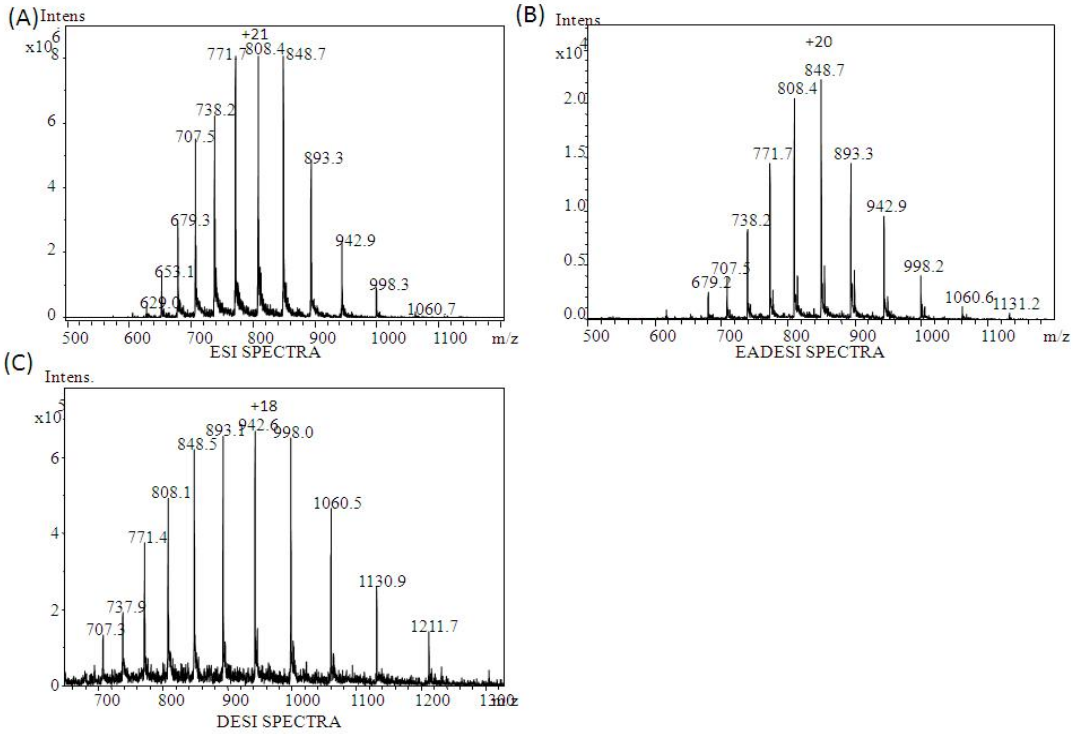

Figure 25. The Spectrum of Myoglobin by (A) ESI (B) EADESI and (C) DESI

DETECTION OF LARGE MOLECULES (ALBUMIN)

Molecular weight of Bovine Serum Albumin (BSA) is 66KDa, it is currently the largest protein measured with ambient ionization methods. Due to the high mass, multiple charged ions are expected.

We tested different experimental conditions for the different concentrations of albumin. Multiple charges of albumin ions were obtained (Figure 26). These ions can include the attachment of H^+, Na^+, and K^+. At present, it is not possible to obtain the spectrum from only one spot; a high quality spectrum must be accumulated and averaged from data from many spots. Therefore, a reliable LOD is difficult to obtain for BSA. We also have difficulty obtaining a good linear relationship between signal intensity and BSA concentration.

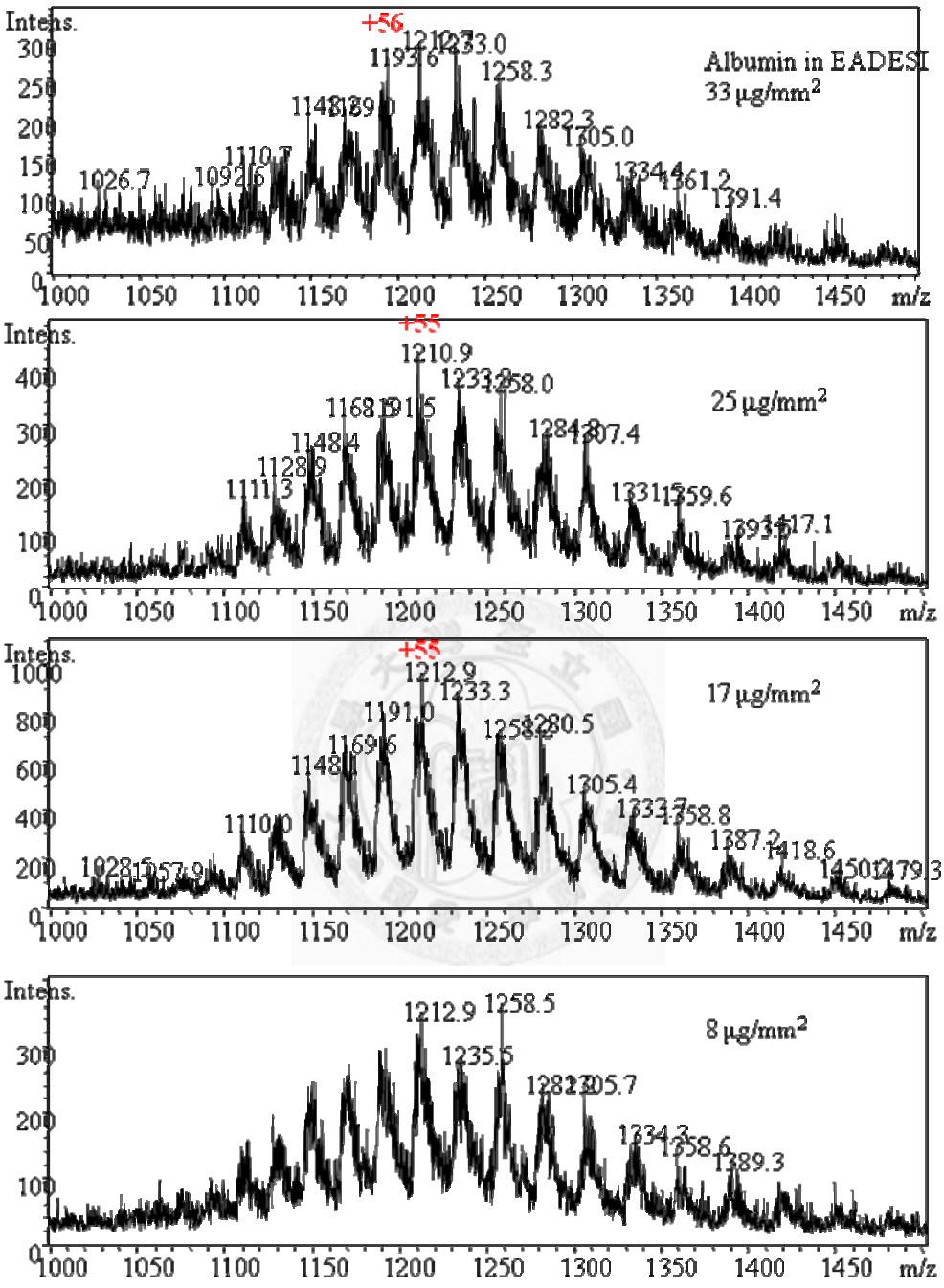

Figure 26. Mass spectra of BSA as a function of concentration

COMPARISON FO AMBIENT IONIZATION METHODS

Table 4[7, 29] is the comparison of the analytical figures of merit, capabilities, and limitations of these emerging methods including several ambient ionization methods and EADESI. Table 4 clearly shows that not all of capabilities for all of the methods have been tested. From the available information it appears that some strength for a particular application using one method may be a weakness in the others.

The strengths of EADESI are limit of detection and the resolution. The resolution of EADESI is the best tested for these ambient ionization methods. In dynamic range and high mass detection terms, EADESI is comparable to the other ambient ionization methods.

For example, the major difference between DESI and EADESI is the resolution. Because of the washing effect, it is difficult to exactly define the resolution of DESI. The resolution of DESI is 200μm. On the other hand, the resolution of EADESI is only 25-50μm.

Table 4. Comparison of Ambient ionization method[7, 29]

Technique	High mass	L.O.D. (f mol)	Dynamic Range	Resolution	Limitations
DESI	66 KDa	1-10	10^3	200μm	Sensitive to the surface; Ill-defined sampling area; analyte washing effect
DART	~1 KDa	7	~20	<3mm	Limited m/z
ELDI	66 KDa	20	N/A	N/A	Sample pretreatment necessary
SSP	15 KDa	1	10^2	635μm	
DBDI	<200	3.5	N/A	N/A	
LAESI	66 KDa	8	10^4	300-400μm	Water rich target needed
DAPPI	<500	56-670	N/A	N/A	
AP IR-MALDI	~3 KDa	1	$10^{1.5}$	40μm	Limited m/z
EADESI	66 KDa	1-30	10^3	25-50μm	

CONCLUSION

EADESI is a novel and simple ambient ionization method. The application of EADESI has been demonstrated for the analysis of proteins, drugs, and human body fluid samples such as urine and blood. The results show the easy desorption of dried solid phase samples by EADESI.

EADESI offers significant advantages as an ambient ionization method such as high spatial resolution and low detection limit. It also has the ability to rapidly analyze complex mixtures with little or no sample preparation. This work has focused on the novel ionization technique, ionization mechanism, high spatial resolution and the similarities and differences among ESI, DESI and EADESI.

In EADESI, the strength of electric field may play an important role in the ionization. Due to the experiment, the distance between the electrode tip and sample plate would be affected by the voltage applied to the tip. The electric field may be measured in the future work.

The difference of detection limit between molecules may be caused by a number of factors, such as the electric permittivity of the protein molecule[30], the spatial distribution of charges[30], different molecular weight[26], solubility[31] etc. All these factors would affect ionization efficiency, and these types of studies could also be performed in the future.

The possible reason of adding matrix can improve detection limit is the attractive force between molecules has changed. Without matrix, ionization efficiency decreased because protein would agglomerate to each other and sample plate. If the sample is mixed with

matrix, the matrix would form a shelter for protein and decreased the attractive force. It may increase the efficiency of desorption.

REFERENCES

1 Venter, A., Nefliu, M. & Cooks, R. G. Ambient desorption ionization mass spectrometry. *TrAC Trends in Analytical Chemistry* **27**, 284-290 (2008).

2 Harris, G. A., Nyadong, L. & Fernandez, F. M. Recent developments in ambient ionization techniques for analytical mass spectrometry. *Analyst* **133**, 1297 - 1301 (2008).

3 Chen, H., Gamez, G. & Zenobi, R. What Can We Learn from Ambient Ionization Techniques? . *Journal of the American Society for Mass Spectrometry* **20**, 1947-1963 (2009).

4 Wiseman, J. M. *et al.* Desorption electrospray ionization mass spectrometry: Imaging drugs and metabolites in tissues. *PNAS* **105**, 18120–18125 (2008).

5 Takáts, Z., Wiseman, J. M., Gologan, B. & Cooks, R. G. Mass Spectrometry Sampling Under Ambient Conditions with Desorption Electrospray Ionization *Science* **306**, 471 - 473 (2004).

6 Weston, D. J. Ambient ionization mass spectrometry: current understanding of mechanistic theory; analytical performance and application areas. *Analyst* **135**, 661 - 668 (2010).

7 Costa, A. B. & Cooks, R. G. Simulated splashes: Elucidating the mechanism of desorption electrospray ionization mass spectrometry. *Chemical Physics Letters* **464**, 1-8 (2008).

8 Venter, A., Sojka, P. E. & Cooks, R. G. Droplet Dynamics and Ionization Mechanisms in Desorption Electrospray Ionization Mass Spectrometry. *Analytical Chemistry* **78**, 8549-8555 (2006).

9 Costa, A. B. & Cooks, R. G. Simulation of atmospheric transport and droplet–thin film collisions in desorption electrospray ionization. *Chem. Commun.*, 3915–3917 (2007).

10 Ifa, D. R., Wu, C., Ouyang, Z. & Cooks, R. G. Desorption electrospray ionization and other ambient ionization methods: current progress and preview. *Analyst* **135**, 669 - 681 (2010).

11 Pasilis, S. P., Kertesz, V. & Berkel, G. J. V. Surface Scanning Analysis of Planar Arrays of Analytes with Desorption Electrospray Ionization-Mass Spectrometry. *Analytical Chemistry* **79** 5956–5962 (2007).

12 Cody, R. B., Laramée, J. A. & Durst, a. H. D. Versatile New Ion Source for the Analysis of Materials in Open Air under Ambient Conditions. *Analytical Chemistry* **77** 2297-2302 (2005).

13 Shiea, J. *et al.* Electrospray-assisted laser desorption/ionization mass spectrometry for direct ambient analysis of solids. *Rapid Communications in Mass Spectrometry* **19**, 3701-3704 (2005).

14 Peng, I. X., Shiea, J., Loo, R. R. O. & Loo, J. A. Electrospray-assisted laser desorption/ionization and tandem mass spectrometry of peptides and proteins. *Rapid Communications in Mass Spectrometry* **21**, 2541-2546 (2007).

15 Peng, I. X., Loo, R. R. O., Shiea, J. & Loo, J. A. Reactive-electrospray-assisted laser desorption/ionization for characterization of peptides and proteins. *Analytical Chemistry* **80**, 6995-7003 (2008).

16 Peng, I. X., Loo, R. R. O., Margalith, E., Little, M. W. & Loo, J. A. Electrospray-assisted laser desorption ionization mass spectrometry (ELDI-MS) with an infrared laser for characterizing peptides and proteins. *Analyst* **135**, 767 - 772 (2010).

17 Na, N. *et al.* Direct Detection of Explosives on Solid Surfaces by Mass Spectrometry with an Ambient Ion Source Based on Dielectric Barrier Discharge. *Journal of Mass Spectrometry* **42**, 1079-1085 (2007).

18 Na, N., Zhao, M., Zhang, S., Yang, C. & Zhang, X. Development of a Dielectric Barrier Discharge Ion Source for Ambient Mass Spectrometry *Journal of the American Society for Mass Spectrometry* **18**, 1859-1862 (2007).

19 Kogelschatz, U., Eliasson, B. & Egli, W. From ozone generators to flat television screens: history and future potential of dielectric-barrier discharges. *Pure Applied Chemistry* **71**, 1819-1828 (1999).

20 Williams, J. P., Patel, V. J., Richard Holland & Scrivens, J. H. The use of recently described ionisation techniques for the rapid analysis of some common drugs and samples of biological origin. *Rapid Communications in Mass Spectrometry* **20**, 1447 - 1456 (2006).

21 Huang, G., Chen, H., Zhang, X., Cooks, R. G. & Ouyang, Z. Rapid screening of anabolic steroids in urine by reactive Desorption Electrospray Ionization. *Analytical Chemistry* **79**, 8327-8332 (2007).

22 Kauppila, T. J. *et al.* Rapid analysis of metabolites and drugs of abuse from urine samples by desorption electrospray ionization-mass spectrometry. *Analyst* **132**, 868 - 875 (2007).

23 Jackson, A. U., Talaty, N., Cooks, R. G. & Berkel, G. J. V. Salt Tolerance of Desorption Electrospray Ionization (DESI). *Journal of the American Society for Mass Spectrometry* **18**, 2218-2225 (2007).

24 Takáts, Z., Wiseman, J. M. & Cooks, R. G. Ambient mass spectrometry using desorption electrospray ionization (DESI): instrumentation, mechanisms and applications in forensics, chemistry, and biology. *Journal of Mass Spectrometry* **40**, 1261 - 1275 (2005).

25 Kertesz, V. & Berkel, G. J. V. Improved imaging resolution in desorption electrospray ionization mass spectrometry. *Rapid Communications in Mass Spectrometry* **22**, 2639 - 2644 (2008).

26 Shin, Y.-S., Drolet, B., Mayer, R., Dolence, K. & Basile, F. Desorption Electrospray Ionization-Mass Spectrometry of Proteins. *Analytical Chemistry* **79** 3514–3518 (2007).

27 Hoffmann, E. d. & Stroobant, V. *Mass Spectrometry: Principles and Applications*. 232 (John Wiley& Sons, Ltd, 2007).

28 Myung, S. *et al.* Coupling desorption electrospray ionization with ion mobility/mass spectrometry for analysis of protein structure: evidence for desorption of folded and denatured States. *JOURNAL OF PHYSICAL CHEMISTRY B* **110**, 5045-5051 (2006).

29 Nemes, P. & Vertes, A. Laser Ablation Electrospray Ionization for Atmospheric Pressure, in Vivo, and Imaging Mass Spectrometry. *Analytical Chemistry* **79**, 8098-8106 (2007).

30 Takáts, Z., Wiseman, J. M., Gologan, B. & Cooks, R. G. Electrosonic Spray Ionization. A Gentle Technique for Generating Folded Proteins and Protein Complexes in the Gas

Phase and for Studying Ion-Molecule Reactions at Atmospheric Pressure. *Analytical Chemistry* **76**, 4050-4058 (2004).

31 Wu, C., Ifa, D. R., Manicke, N. E. & Cooks, R. G. Rapid, Direct Analysis of Cholesterol by Charge Labeling in Reactive Desorption Electrospray Ionization. *Analytical Chemistry* **81**, 7618-7624 (2009).

1